downstream of the three cylinders at the intermediate spacing ($1.5 < L/D \leq 3.0$). Fig. 4 shows the typical flow structures for two different configurations [(L/D, θ) = (2.5, 10°) and (2.5, 30°)], in terms of contours of instantaneous vorticity. At the intermediate spacing, the gap flow going through the cylinders has enough momentum to be biased in the near wake; as such the downstream cylinders may have relatively narrow and wide wakes. For (L/D, θ) = (2.5, 10°) (Fig. 4a), the near wake of the upstream cylinder 1 is completely suppressed by the downstream cylinders 2 and 3; the gap flow is biased toward the lower cylinder 3. As a result, the downstream cylinders 2 and 3 generate relatively wide and narrow wakes, respectively. Further downstream, the inner shear layers associated with the gap flow are enveloped by the vortices formed on the lower side of cylinder 3, while counter-signed vortices shed from the upper side of cylinder 2. Therefore, only a vortex street is produced, with distinct frequencies of vortex shedding from the upper and lower sides of the three-cylinder configuration.

For (L/D, θ) = (2.5, 30°) (Fig. 4b), the downstream cylinder 2 is totally submerged in the wake of the upstream cylinder 1. In other words, the shear layers separating from the upstream cylinder 1 overshoot the downstream cylinder 2 and roll up into vortices downstream of cylinder 2. However, the gap flow, which is biased toward cylinder 3, results in a relatively narrow wake for cylinder 3 and a relatively wide wake for cylinder 2. Again, the inner shear layers associated with the gap flow are enveloped by the vortices formed on the lower side of cylinder 3. Therefore, only one vortex street is generated, which is similar to the configuration with a smaller θ (Fig. 4a).
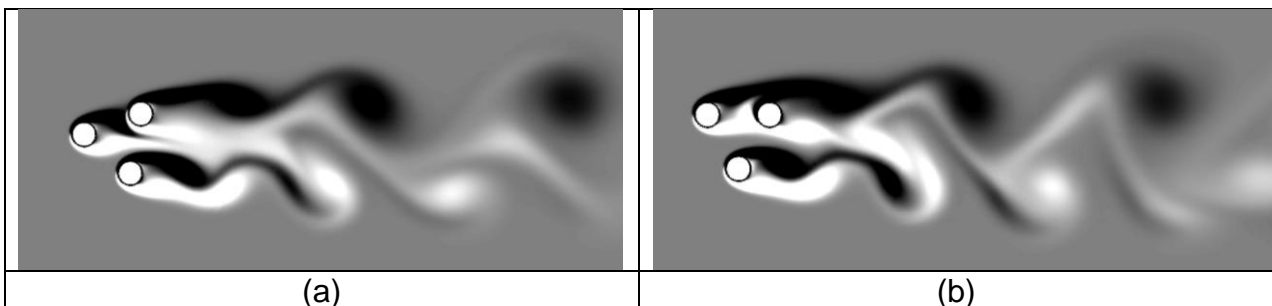

| (a) | (b) |

Fig. 4 Contours of instantaneous vorticity in the near wake of the three cylinders at (a) (L/D, θ) = (2.5, 10°) and (b) (L/D, θ) = (2.5, 30°).

3.3 Two streets of vortices

At the large spacing $3.0 < L/D \leq 4.0$ and $\theta < 50°$, the group of three cylinders produces a wake consisting of two streets of vortices. Fig. 5 shows the typical flow structures for two different configurations [(L/D, θ) = (4.0, 0°) and (4.0, 30°)], in terms of contours of instantaneous vorticity. For (L/D, θ) = (4.0, 0°) (Fig. 5a), the three-cylinder configuration is symmetric about the horizontal line going through the center of the configuration. The shear layers separating from the upstream cylinder 1 are confined by the downstream side-by-side cylinders 2 and 3, and thus there is no vortex rolling up in the gap. Meanwhile, each of the downstream cylinders generates a Karman vortex street, with the vortex shedding from the two cylinders appearing an

anti-phase fashion. Therefore, the pattern of counter-signed vortices appears symmetric about the horizontal line going through the center of the configuration.

For $(L/D, \theta) = (4.0, 30^o)$ (Fig. 5b), cylinder 1 and cylinder 2 are in a tandem arrangement while cylinder 3 is located on the lower side of cylinders 1 and 2. The large spacing between cylinder 1 and cylinder 2 allows the upstream cylinder 1 to generate its near wake of shedding vortices. The reattachment of the vortices from the upstream cylinder 1 triggers vortices shedding from the downstream cylinder 2 and, consequently, there is one Karman vortex street downstream of the tandem cylinders 1 and 2. Cylinder 3 also produces a Karman vortex street. Therefore, this configuration of the three cylinders has a near wake of two streets of vortices.
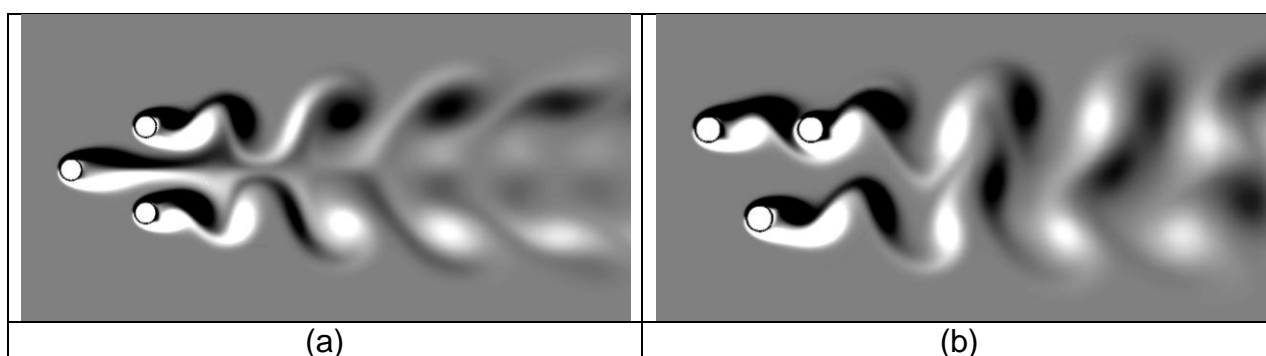

| (a) | (b) |

Fig. 5 Contours of instantaneous vorticity in the near wake of the three cylinders at (a) $(L/D, \theta) = (4.0, 0^o)$ and (b) $(L/D, \theta) = (4.0, 30^o)$.
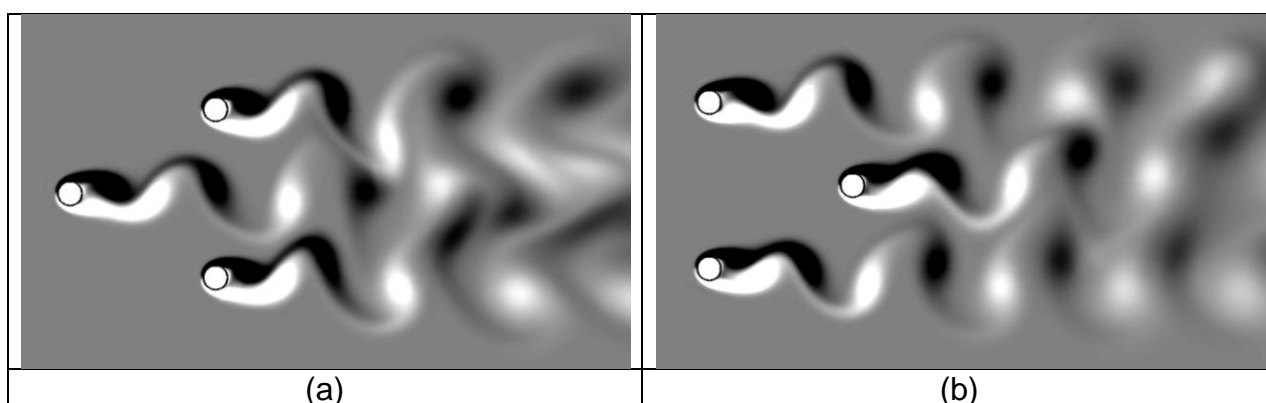

| (a) | (b) |

Fig. 6 Contours of instantaneous vorticity in the near wake of the three cylinders at (a) $(L/D, \theta) = (7.0, 0^o)$ and (b) $(L/D, \theta) = (7.0, 60^o)$.

3.4 Three streets of vortices

For the symmetric configurations ($\theta = 0^o$ and 60°) of the three cylinders at the large spacing $L/D > 4.0$, a near wake of three streets of vortices is generated. Fig. 6 shows the flow structures for $(L/D, \theta) = (7.0, 0^o)$ and $(7.0, 60^o)$, in terms of contours of instantaneous vorticity. It can be seen that each of the three cylinders generates a

Karman vortex street. The street of vortices in the middle interacts with the other two streets of vortices as they evolve downstream.
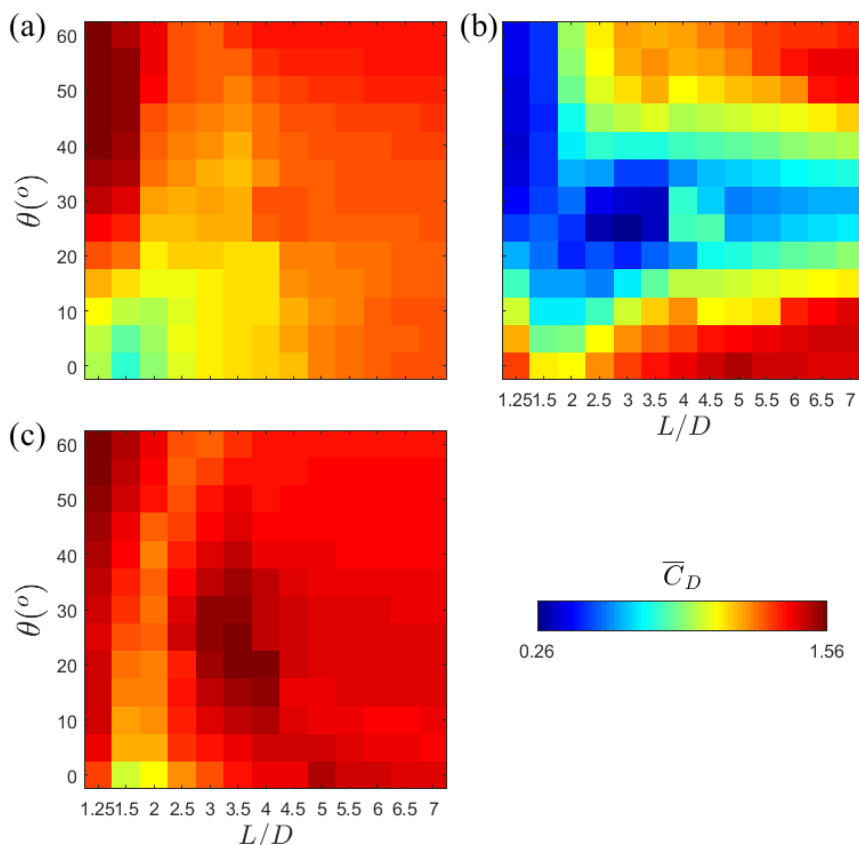

Fig. 7 Dependence of time-mean drag force ($\overline{C}_D$) on (*L/D*, θ) for cylinder 1 (a), cylinder 2 (b) and cylinder 3 (c).

4. FLUID FORCES

4.1 Time-mean forces

Time-mean drag and lift forces acting on the individual cylinders are presented in Figs. 7 and 8, respectively, in terms of contours of force coefficients in the (*L/D*, θ) plane. This provides a global view of the dependence of fluid forces on the three-cylinder configurations.

In Fig. 7, the maximum drag coefficient ($\overline{C}_D$) is identified at (*L/D*, θ) = (1.25, 50°) for cylinder 1 and at (*L/D*, θ) = (3.5, 20°) for cylinder 3, while the minimum $\overline{C}_D$ is detected at (*L/D*, θ) = (3.0, 25°) for cylinder 2.

In Fig. 8, it can be seen that cylinder 1 and cylinder 3 are associated with time-mean lift forces with large magnitude at the small spacing ($L/D < 1.5$). The positive lift force (along the positive y-direction) is acting on cylinder 1, while the negative lift force (along the negative y-direction) is acting on cylinder 3. That is, cylinder 1 and cylinder 3 are repelled by the opposite lift forces. For cylinder 2, at the intermediate spacing 2.5

$< L/D < 4.0$ the lift force switches from negative to positive as the incident angle θ is increase from 10° to 50°.
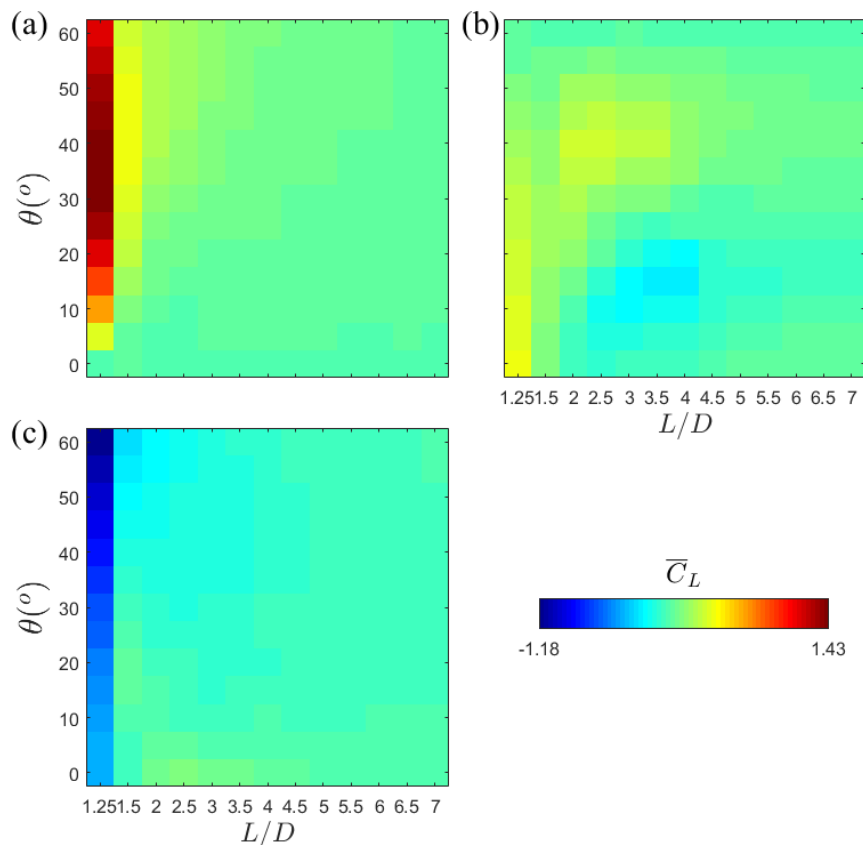

Fig. 8 Dependence of time-mean lift force ($\overline{C}_L$) on (L/D, θ) for cylinder 1 (a), cylinder 2 (b) and cylinder 3 (c).

4.2 Fluctuating forces

The fluctuating drag and lift forces on the three cylinders are presented Figs. 9 and 10, respectively. At the small spacing $L/D \leq 1.25$, all three cylinders are associated with large fluctuating drag forces (C_D'). At the large spacing $L/D > 4.0$, there is a large fluctuating drag force on cylinder 2 throughout the range of incident angle. This cylinder is also associated with a large fluctuating lift force at the large spacing $L/D > 4.0$ and $20^o < \theta < 40^o$ (Fig. 10b).

5. CONCLUSIONS

A systematic numerical simulation study was conducted at a low Re = 100 to investigate the flow structures and fluid forces of the three cylinders arranged in an equilateral triangular form. The spacing between adjacent cylinder was from L/D = 1.25-7.0 while the incident angle was changed from $\theta = 0^o$ to 60° (covering all possible orientation configurations). It has been observed that flow structures in the near wake

of the three-cylinder configuration, time-mean and fluctuating fluid forces on the individual cylinders strongly depend on (L/D, θ). The three-cylinder configuration generates a single Karman vortex street, a deflected near wake, or two or three streets of vortices in the near wake, depending on (L/D, θ). Furthermore, there is a close correlation between the near wake behaviour and the fluid forces observed.
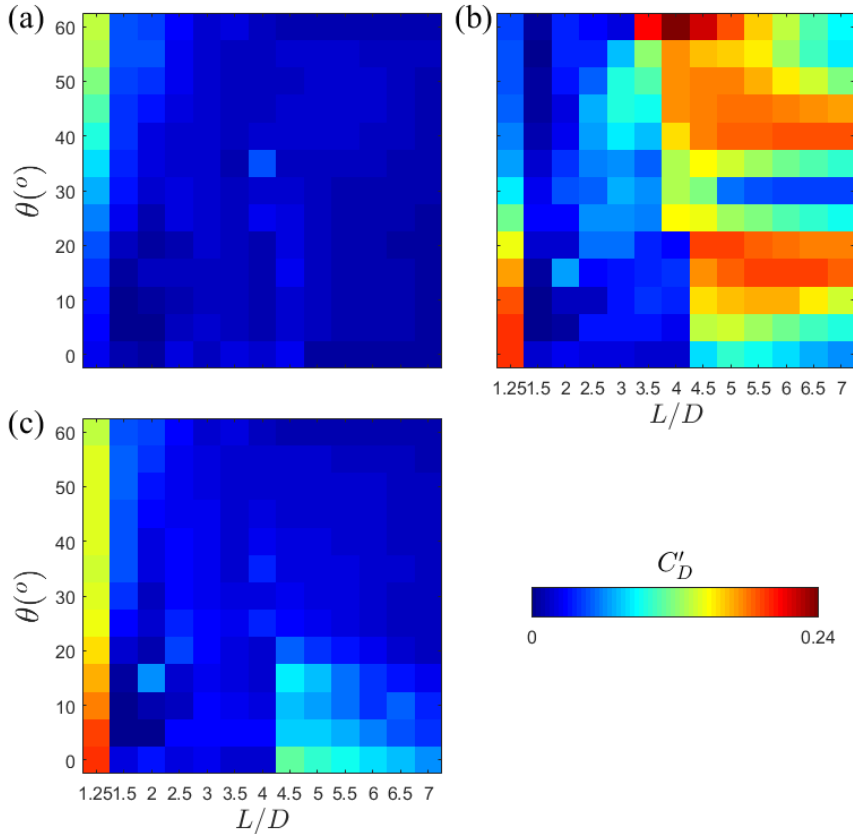

Fig. 9 Dependence of fluctuating drag force ($C_D^{'}$) on (L/D, θ) for cylinder 1 (a), cylinder 2 (b) and cylinder 3 (c).
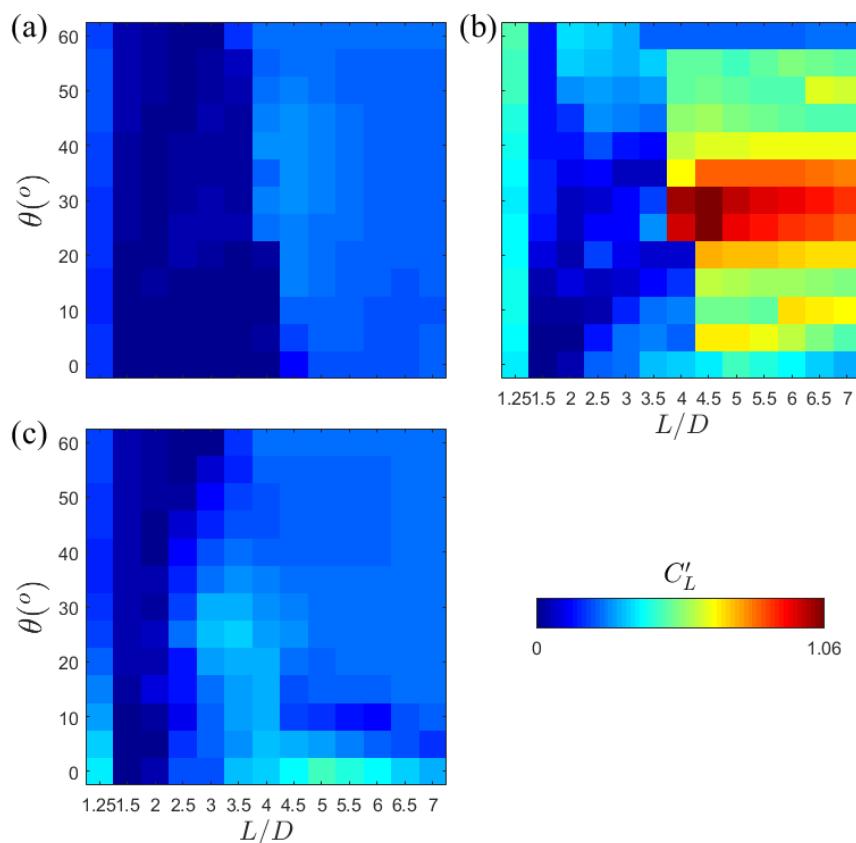
Fig. 10 Dependence of fluctuating lift force (C_L') on (L/D, θ) for cylinder 1 (a), cylinder 2 (b) and cylinder 3 (c).

REFERENCES

Alam, M.M., Bai, H.L. and Zhou, Y. (2016), "The wake of two staggered square cylinders", *J. Fluid Mech.*, **801**, 475-507.

Bao, Y., Zhou, D. and Huang, C. (2010), "Numerical simulation of flow over three circular cylinders in equilateral arrangements at low Reynolds number by a second-order characteristic-based split finite element method", *Comp. Fluids*, **39**, 882-899.

Gu, Z. and Sun, T. (2001), "Classification of flow pattern on three circular cylinders in equilateral-triangular arrangements', *J. Wind Eng. Indust. Aerodyn.* **89**, 553-568.

Han, P., Pan, G. and Tian, W. (2018), "Numerical simulation of flow-induced motion of three rigidly coupled cylinders in equilateral-triangle arrangement", *Phys. Fluids*, **30**, 125107.

Lam, K. and Cheung W.C. (1988), "Phenomena of vortex shedding and flow interference of three cylinders in different equilateral arrangements", *J. Fluid Mech.*, **196**, 1-26.

Tatsuno, M., Amamoto, H. and Ishi-I, K. (1998), "Effects of interference among three equidistantly arranged cylinders in a uniform flow", *Fluid Dyn. Research.*, **22**, 297-315.

Wang, H., Yu, G. and Yang, W. (2013), "Numerical study of vortex-induced vibrations of three circular cylinders in equilateral-triangle arrangement", *Advan. Mech. Eng.*, **2013**, 287923.

Zdravkovich, M.M. (1977), "Review of flow interference between two circular cylinders in various arrangements", *J. Fluids Eng.* **99**, 618-633

Zhou, Y. and Alam, M.M. (2016), "Wake of two interacting circular cylinders: A review", *Int. J. Heat Fluid Flow*, **62**, 510-537.